Na$^+$/Li$^+$-ionic conductivity in Fe$_2$Na$_2$K[Li$_3$Si$_{12}$O$_{30}$]

B. Röska[a], I. Akter[a], M. Hoelzel[b], S.-H. Park[a],*

[a] Department of Geo- and Environmental Sciences, Section of Crystallography, Ludwig-Maximilians-Universität München (LMU), Munich, Germany
[b] Heinz Maier-Leibnitz Zentrum (MLZ), Technische Universität München (TUM), Garching, Germany

ARTICLE INFO

ABSTRACT

A sugilite-type double 6-membered ring (D6MR) silicate, Fe$_2$Na$_2$K[Li$_3$Si$_{12}$O$_{30}$] could be obtained for the first time under mild hydrothermal conditions. Impedance spectra revealed a bulk conductivity of 1.2×10^{-5} S cm^{-1} at 923 K. Hopping pathways of Li$^+$ and Na$^+$ were indicated in difference Fourier (ΔF) maps parallel to the D6MRs network using neutron powder diffraction at 298–1123 K. The current study presents a promising prototype for combined 2-dimensional Li$^+$/Na$^+$-ionic conductors with crystal-chemical flexibility and thermally high stability.

1. Introduction

In exploring prototype structures for direction-dependent design and engineering of all-solid-state electrochemical cells, our attention was taken to the so-called sogdianite-sugilite series as promising stable high-temperature ionic conductors [1]. This consideration is based on the interesting structural property of this solid solution: the 3-dimensional (3D) topology stable up to about 1300 K with 2-dimensional (2D) anisotropic properties in the hexagonal metric (a ≈ 10 Å and c ≈ 14 Å; **P**6/mcc). This geometrical flexible 3D structure type belongs to the milarite group showing an extremely wide range of chemical compositions, which is comparable to those of spinels and perovskites. Its high compositional diversity, as given in Table 1, is represented by the general formula for the milarite family $^{[6]}A_2$ $^{[9]}B_2$ $^{[12]}C$ $^{[18]}$D $[^{[4]}T23^{[4]}T1_{12}O_{30}]$ [1-8]. Characteristically, D6MRs of [$T1$O$_4$] tetrahedra form channels running along the **c** axis (Fig. 1). Perpendicular to this, the layers of alternating, highly distorted [$T2$O$_4$] tetrahedra and [AO$_6$] octahedra build up a rugged framework with a high degree of crystal-chemical flexibility (Fig. 1b) [9]. In between two such network layers, the nine-fold coordinated B site is bounded in by two [AO$_6$] octahedra. The twelve-fold coordinated C site is found at the axis of the channels, wedged in between two D6MRs. Centred within the D6MRs, the eighteen-fold coordinated D site is mostly unoccupied [9]. In this sense, the milarite-type topology can be regarded as a pseudo-porous framework with 6MR-openings which are too small for reversible hydration-dehydration process, hence stable against moisture. A low sensitivity to thermal variation and hydration but with a high chemical flexibility for solid solution formation is one of the most relevant prerequisites in development of economically-ecologically friendly electrochemical materials.

For this purpose, the current study presents synthesis and characterisation of the synthetic counterpart of the mineral sugilite rarely occurring. Typically, natural sugilite samples from a few known deposits [2,10,11] are described by the generic formula (Fe^{3+}, Al, Mn^{3+})$_2$Na$_2$K[Li$_3$Si$_{12}$O$_{30}$] [4]. The Zr-rich counter part sogdianite ((Zr, Ti, Fe^{3+}, Al)$_2$(Na, □)$_2$K[Li$_3$Si$_{12}$O$_{30}$] [1]) possesses considerably less Na for the presence of quadrivalent cations at the A site. In spite of the same amount of Li per formula unit (pfu) in sugilite and sogdianite, the former shows a much higher ionic conductivity mainly due to the high amount of mobile Na$^+$. Hence, sugilite is considered as an interesting combined Li$^+$/Na$^+$-ion conductor. An extensive study of Li$^+$/Na$^+$ dynamics in the mineral sugilite will be reported elsewhere. We focus here on the investigation of sugilite analogue, Fe$_2^{3+}$ Na$_2$K[Li$_3$Si$_{12}$O$_{30}$] synthesized under mild hydrothermal conditions. The synthetic products were subject to variable-temperature impedance spectroscopy and high-resolution neutron powder diffraction (HRNPD). Subtle structure analysis and subsequent inspection of difference Fourier (ΔF) maps resolved the dynamic disorder of Li and Na. Their 2D hopping paths are strongly anisotropic perpendicular to [001] direction.

2. Experimental

2.1. Hydrothermal synthesis

Hydrothermal syntheses were performed with varying starting compositions in alkali environment to enhance the solubility of α-Fe$_2$O$_3$ and SiO$_2$ in the starting suspension. As given in Table 2, a series of synthesis mixtures were prepared with different ratios of

* Corresponding author.
  E-mail address: sohyun.park@lmu.de (S.-H. Park).

Table 1
Possible cation occupation at the respective sites in milarite-type structure, revealing the broad crystal-chemical flexibility (□=vacancy) [1,4,12].

Sites	Multiplicity	Coordination	Element
T1	24	4	Si, Al
T2	6	4	Li, Be, B, Mg, Al, Si, Mn^{2+}, Zn
A	4	6	Al, Fe^{3+}, Sn^{4+}, Mg, Zr, Fe^{2+}, Ca, Na, Y, Sc, Mn^{3+}, Ti^{4+}
B	4	9	Na, H_2O, □, K
C	2	12	K, Na, Ba, □
D	2	18	□

Table 2
Molar ratios of the educts in reaction gels and quantitative phase analysis using multipattern Rietveld analyses with XPD data of selected syntheses products (S: $Fe_2Na_2K[Li_3Si_{12}O_{30}]$; Qz: α-quartz; H: α-Fe_2O_3).

Molar ratios of educts Na: Fe: K: Li: Si: H_2O	Syntheses Products S: Qz: H [wt %]
1: 2: 1: 3: 12: 1000	93.1(5): 6.8(1): 0.0(1)
1: 2: 1: 3: 10: 1000	92(1): 5.4(3): 3.0(3)
1: 2: 1: 3: 10: 500	63.0(3): 29(1): 8.0(5)
1: 2: 1: 3: 7: 1000	86(1): 13.6(2): 0.1(1)
1: 1.5: 1: 3: 7: 1000	90(1): 8.6(2): 1.3(1)
1: 1.2: 1: 3: 7: 1000	88(2): 11.5(5): 0.0(0)
1: 1: 1: 3: 7: 1000	94.6(5): 0.0(0): 5.4(1)
1: 0.9: 1: 3: 7: 1000	92.1(3): 0.0(0): 7.9(2)
1: 0.8: 1: 3: 7: 1000	91.3(6): 0.5(1): 8.2(1)

reaction educts, i.e. NaOH (99%, *Riedel-de Haen AG*), LiOH·H_2O (56.6%, *Alfa Aesar*), KOH (85%, *Merck*), Fe_2O_3 (*Merck*), SiO_2 colloidal dispersion (40 wt% in H_2O, *Alfa Aesar*). These were added step-by-step to deionized H_2O while vigorously stirring. The starting gel was aged further for 4 h at room temperature (RT) and brought to the reaction under hydrothermal conditions in Teflon-lined steel autoclaves at 500 – 540 K for 5 – 14 days. The synthesis products were washed with deionized water and dried overnight at RT.

2.2. X-ray powder diffraction (XPD)

For phase identification of synthetic product XPD data were collected on a powder diffractometer (STOE STADI P) using Mo $K\alpha_1$ radiation (Ge(111) monochromator) in Debye-Scherrer transmission geometry. XPD data was collected in a wide 2θ range of 2–75° on a linear position-sensitive detector (PSD) with a step with of 0.02° (2θ). For the use in Rietveld analysis several XPD data sets were added up to improve counting statistics. Rietveld calculations were performed with the software package FullProf Suite [13].

2.3. High resolution neutron powder diffraction (HRNPD)

HRNPD was conducted at the instrument SPODI [14] at the neutron facility FRM2, Garching near Munich, Germany. Using a wavelength of 1.463 Å (Ge(551) monochromator) a set of HRNPD data was collected on 80 vertically aligned PSDs with 300 mm high collimators. A powder sample (about 1 g) was packed into a Nb can and positioned within a Nb high-temperature (HT) furnace under vacuum. Data acquisition was made at 298 K, 573 K, 723 K, 923 K, and 1123 K, subsequently. A 2θ range of 1–160° in steps of 0.05° was recorded several times at each measuring temperature and summed up to increase the signal/noise ratio. With results from structure refinements with HRNPD data sets, ΔF maps, and bond valence sums (BVS) were evaluated using FullProf Suite [13]. BVS values with estimated standard deviations are derived from individual bonding distances of the refined structure model [15].

2.4. Impedance spectroscopy (IS)

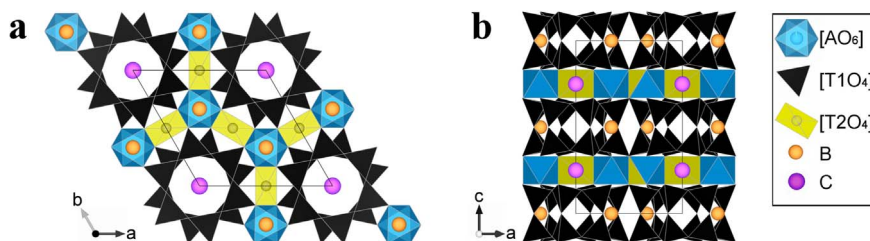A disc of 2 mm thickness and a radius of 2 mm (A = 12.56 mm²) was pressed with the selected sample. The flattened disc surface area was covered with Pt paste and tempered at 473 K to remove organic glue. The disc was locked between two Pt electrodes and brought into a home-constructed HT probe to acquire complex impedance spectra using a *Hewlett Packard 4284A* LCR meter. A NiCr-Ni thermocouple located immediately next to the sample (0.3 mm) was connected to a temperature controller maintaining a constant sample temperature with the accuracy of ±1 K±. For data evaluation with less grain boundary effect, we used the IS spectra recorded at cooling from 963 K down to RT in steps of 30 K in the frequency interval of 20 Hz to 1 MHz. We want to stress that the sample contained the minor phase α-Fe_2O_3 (5.3(1) wt%), but the intrinsic electron conductivity of α-Fe_2O_3 is out of the energy window probed [16,17].

3. Results and discussion

3.1. Syntheses products and phase analysis

As-synthesized products in a form of disc consisted of reddish fine crystallites rimmed with some coarse white agglomerates. According to XPD patterns, these white aggregates comprised crystalline $Li_2Si_2O_5$ and SiO_2 (α-quartz type), but they could easily be detached from the main phase segregation. Multi pattern Rietveld refinements with XPD data of the main product part (Fig. 2) agreed with the sugilite-type phase given in Ref. [4], i.e. $Fe_2Na_2K[Li_3Si_{12}O_{30}]$.

In general, the content of quartz was suppressed by lowering the amount of Si in the starting gel. A tiny decrease of Fe_2O_3 in the reaction gel dramatically suppressed the formation of sugilite-type phase. Slight increments of NaOH, LiOH, or KOH concentrations, the HT aging of the starting suspension (320 K Ref. [18]), or the extension of aging period longer than 24 h at RT lead to the formation of $Li_2Si_2O_5$ as the main product. A short ageing time of 1 h gave rise to mixtures of undesired phases, such as $Li_6Si_2O_7$, Na_5FeO_4, $KFeSi_3O_8$ and $Li_2Si_2O_5$. Higher synthesis temperatures of 510–540 K favoured the formation of α-Fe_2O_3. The highest portion of sugilite-type phase was obtained from the staring mixture with the molar ratios Na:K:Fe:Li:Si:H_2O = 1:1:1:3:7:1000 in excess of Si, Li, K with respect to the ideal Fe-rich sugilite end-member composition (Table 2).

No single crystals of $Fe_2Na_2K[Li_3Si_{12}O_{30}]$ large enough for single

Fig. 1. Tetrahedral-octahedral framework topology of milarite-type compounds, plotted in [001] (a) and in [210] (b), where *A*=Fe^{3+}, *B*=Na, *C*=K, *T1* = Si, and *T2* = Li in $Fe_2Na_2K[Li_3Si_{12}O_{30}]$.